International Journal of Modern Physics D, Vol. 6, No. 2 (1997) 125–142

COSMIC IRON WHISKERS: THEIR ORIGIN, LENGTH DISTRIBUTION AND ASTROPHYSICAL CONSEQUENCES

J. V. NARLIKAR
Inter-University Centre for Astronomy and Astrophysics, Post Bag 4, Ganeshkind, Pune 411 007, India

N. C. WICKRAMASINGHE
University of Wales Cardiff, School of Mathematics, Senghennydd Road, Cardiff CF2 4AG, UK

R. SACHS
Max-Planck-Institut für extraterrestrische Physik, Giessenbachstrasse, 85740 Garching, Germany

F. HOYLE
102 Admirals Walk, West Cliff Road, West Cliff, Bournemouth, Dosset BH2 5HF, UK

Received 2 November 1996
Revised 20 January 1997

The idea that iron ejected from supernovae condenses in the form of slender whiskers is developed further. The formation mechanism and the resulting length distribution of the whiskers are related to several astrophysical and cosmological phenomena.

1. Introduction

A few years ago two of us (Hoyle and Wickramasinghe[1]) had advanced the hypothesis that the iron synthesized in massive stars and ejected in supernova explosions would condense from a vapour state into long and slender grains shaped like whiskers. Although the notion of a whisker-shaped grain appears unusual against the common expectation of a roughly spherical particle of dust, the above paper made out a plausible case for it, based on the physics of condensation and growth of metallic vapours and the optical properties of such condensates.

In the present paper we explore that idea further in the light of several observations in galactic and extragalactic astronomy where the whisker shaped grains can successfully account for features that cannot otherwise be easily explained. These features include far infrared absorption dips in the spectrum of Crab Pulsar, a depression in the far infrared CII line strengths at the galactic centre, the efficient

and hence more economic mode of absorption and re-emission of high frequency radiation in high redshift objects, the possible resolution of an enigma associated with the centimetre radiation of high redshift radio sources and the thermalization of cosmological radiation fields into a microwave background.

We claim that a menu as varied as this demonstrates the viability and richness of an idea which possesses the further attraction that it has a basis in laboratory experiments on condensation of metallic vapours and can be tested by more detailed observations of a variety of astronomical sources.

Before dealing with the observational aspects we briefly go through the theoretical aspects of the model. In the following section we discuss the theory of formation and growth of the whiskers and their equilibrium distribution with respect to length. We next discuss the optical properties of individual whiskers and the mean mass absorption coefficient that is appropriate for an equilibrium length distribution. The model is then applied to the different scenarios referred to above.

2. Theory of Iron Whisker Growth

Iron is a major product of stellar nucleosynthesis that is ejected in a supernova explosion. For a Type II supernova exemplified by SN1987A the total mass of iron produced is close to $0.1M_{\odot}$ per supernova. An iron rich shell of initial radius 10^9 cm, density 10^9 g cm^{-3} and temperature 10^{10}K expands adiabatically, cooling as it does so. The stable condensation and growth of iron in the solid phase occurs only after the decay of Ni^{56} to Fe^{56} (which continues in the shell) is nearly completed. Higher temperature condensates such as aluminium oxide which are less abundant[2] would initially become dissociated due to a rise of gas temperature to some 10,000K that would be caused by the radioactive decay of Ni^{56} (Ref. 1). The nucleation and growth of iron particles is estimated to occur at a radial distance of $R = 10^{16}$ cm when the ambient density has fallen to 10^{-15} g cm^{-3} and the temperature is $T = 1000$K. Initial growth occurs as spherical condensation nuclei, the growth proceeding thus until a radius of 0.01μm is reached, when each aggregate experiences a radioactive decay of Co^{56} which has a half-life of 78 days (see Ref. 1). These decays define disclocation axes along which whisker growth may subsequently take place. There is considerable laboratory evidence that metal particles condensing from a tenous cooling vapour do indeed tend to grow in whisker form.[3–5] Whisker growth from an initial length of 0.01μm proceeds according to the formula.[6]

$$l = l_0 \exp t/t_1 \tag{1}$$

where l is the length, t is the time and t_1 is a time constant defined by

$$t_1 = (2mn\nu\alpha/as)^{-1} \tag{2}$$

Here m is the atomic mass and n is the number density of Fe, ν is the thermal speed, α is the sticking coefficient, a is the initial radius and s is the density of bulk

iron. With appropriate values for these parameters ($\nu = 3.9 \times 10^4$ cm/s, $\alpha = 0.1$, $s = 7.8$ g/cm^3), it can be shown that $t_1 = 10^6$s. With $l_0 = 2a = 0.02\mu$m the time to grow to $l = 1$mm is then 1.1×10^7s. It can be shown that this is close to the limiting length defined by the condition that an impinging atom can migrate to the growing tip during the time-interval between two successive collisions.

These considerations apply to condensation in an approximately isothermal shell at a temperature that remains close to the saturation value. In such circumstances whisker growth would not be halted by depletion of the ambient iron vapour.

Not all the whiskers would grow to the full length of ~ 1 mm, however. A length distribution can be derived if we assume that nuclei with appropriate dislocation axes for whisker growth arise with equal probability throughout a condensation time t_c. If N refers to the total number of whiskers at time $t < t_c$, then

$$dN = Adt \tag{3}$$

where A is a constant. Also from (1) we have

$$dl = (1/t_1)ldt \tag{4}$$

so that from (3) and (4) we obtain

$$dN = \text{const. } dl/l \tag{5}$$

The differential length distribution arising from the formation process can therefore be written in the form

$$ndl = Bdl/l\,, \qquad l_{\min} < l < l_{\max} \tag{6}$$

where ndl denotes the number of whiskers with lengths in the range l, $l + dl$, and $l_{\min}$, $l_{\max}$ refer to the minimum and maximum lengths of the whiskers.

It is of interest to note that the distribution (6) also corresponds to an equipartition of mass of whiskers with respect to length, and such a size distribution might be maintained naturally from whisker fragmentation processes. However, as we will see in the following section, the upper limit of the distribution will depend on the driving mechanism that may push the grains from their local site of origin out to greater distances.

3. Mean Mass Extinction Coefficients

The electromagnetic absorption and scattering properties of iron needles of radius 0.01μm and with lengths distributed according to (6) could be calculated using a combination of the usual Mie-type formulae for infinite cylinders with the appropriate Rayleigh formulae for highly elongated prolate spheroids.[7,8] Using procedures described earlier for calculating optical constants of iron at long wavelengths,[6] together with laboratory data for refractive and absorptive indices at wavelengths less than 10 micrometres, we compute the mass extinction coefficient for randomly oriented iron needles of radius 0.01μm and length distributed according to (6) with various cut-off lengths $l_{\min}$, $l_{\max}$. Thus we have

$$\bar{\kappa} = \frac{1}{(l_{\max} - l_{\min})} \int_{l_{\min}}^{l_{\max}} \kappa dl \tag{7}$$

for a number of values of $l_{\min}$. (The integrand represents the total cross-section for particles in the length range l, $l + dl$). We considered realistic values of $l_{\min}$ in the range 3–10μm, but found that the resulting mean opacities are not sensitive to the precise value adopted, because of the convergence of the integral at the lower integration limit. The results of the calculations are given in Table 1 and shown in Fig. 1.

Table 1. Mass absorption coefficient as a function of wavelength λ for a distribution $n \sim 1/l$ and $10\mu\text{m} \leq l \leq l_{\max}$.

$\lambda[\mu\text{m}]$	$l_{\max}[\mu\text{m}]$		$\kappa[\text{cm}^2\text{g}^{-1}]$	
	50	100	500	1000
3.67×10^{-1}	6.11×10^{4}	6.11×10^{4}	6.11×10^{4}	6.11×10^{4}
4.06×10^{-1}	6.75×10^{4}	6.75×10^{4}	6.75×10^{4}	6.75×10^{4}
4.45×10^{-1}	7.44×10^{4}	7.44×10^{4}	7.44×10^{4}	7.44×10^{4}
4.71×10^{-1}	7.85×10^{4}	7.85×10^{4}	7.85×10^{4}	7.85×10^{4}
5.10×10^{-1}	8.31×10^{4}	8.31×10^{4}	8.31×10^{4}	8.31×10^{4}
5.49×10^{-1}	8.52×10^{4}	8.52×10^{4}	8.52×10^{4}	8.52×10^{4}
6.01×10^{-1}	8.59×10^{4}	8.59×10^{4}	8.59×10^{4}	8.59×10^{4}
6.53×10^{-1}	8.56×10^{4}	8.56×10^{4}	8.56×10^{4}	8.56×10^{4}
6.92×10^{-1}	8.46×10^{4}	8.46×10^{4}	8.46×10^{4}	8.46×10^{4}
8.10×10^{-1}	8.56×10^{4}	8.56×10^{4}	8.56×10^{4}	8.56×10^{4}
1.03×10^{0}	8.01×10^{4}	8.01×10^{4}	8.01×10^{4}	8.01×10^{4}
1.31×10^{0}	8.14×10^{4}	8.14×10^{4}	8.14×10^{4}	8.14×10^{4}
1.67×10^{0}	7.22×10^{4}	7.22×10^{4}	7.22×10^{4}	7.22×10^{4}
2.16×10^{0}	5.85×10^{4}	5.85×10^{4}	5.85×10^{4}	5.85×10^{4}
5.00×10^{0}	6.42×10^{4}	6.42×10^{4}	6.42×10^{4}	6.42×10^{4}
1.00×10^{1}	6.49×10^{4}	6.49×10^{4}	6.49×10^{4}	6.49×10^{4}
2.00×10^{1}	1.72×10^{5}	1.72×10^{5}	1.73×10^{5}	1.72×10^{5}
3.00×10^{1}	3.11×10^{5}	3.16×10^{5}	3.19×10^{5}	3.19×10^{5}
5.00×10^{1}	5.88×10^{5}	6.57×10^{5}	7.04×10^{5}	7.08×10^{5}
1.00×10^{2}	9.17×10^{5}	1.64×10^{6}	2.17×10^{6}	2.16×10^{6}
2.00×10^{2}	2.68×10^{5}	2.60×10^{6}	6.48×10^{6}	6.52×10^{6}
3.00×10^{2}	1.19×10^{5}	1.39×10^{6}	1.08×10^{7}	1.19×10^{7}
5.00×10^{2}	4.28×10^{4}	5.05×10^{5}	1.95×10^{7}	2.28×10^{7}
1.00×10^{3}	1.07×10^{4}	1.27×10^{5}	2.36×10^{7}	4.09×10^{7}
2.00×10^{3}	2.67×10^{3}	3.17×10^{4}	1.03×10^{7}	4.39×10^{7}
3.00×10^{3}	1.19×10^{3}	1.41×10^{4}	5.12×10^{6}	3.31×10^{7}
5.00×10^{3}	4.28×10^{2}	5.08×10^{3}	1.98×10^{6}	1.83×10^{7}
1.00×10^{4}	1.07×10^{2}	1.27×10^{3}	5.08×10^{5}	6.16×10^{6}
2.00×10^{4}	2.67×10^{1}	3.17×10^{2}	1.28×10^{5}	1.70×10^{6}
3.00×10^{4}	1.19×10^{1}	1.41×10^{2}	5.71×10^{4}	7.71×10^{5}
5.00×10^{4}	4.28×10^{0}	5.08×10^{1}	2.05×10^{4}	2.80×10^{5}
1.00×10^{5}	1.07×10^{0}	1.27×10^{1}	5.15×10^{3}	7.04×10^{4}
3.00×10^{5}	1.19×10^{-1}	1.41×10^{0}	5.72×10^{2}	7.83×10^{3}
1.00×10^{6}	1.07×10^{-2}	1.27×10^{-1}	5.15×10^{1}	7.05×10^{2}

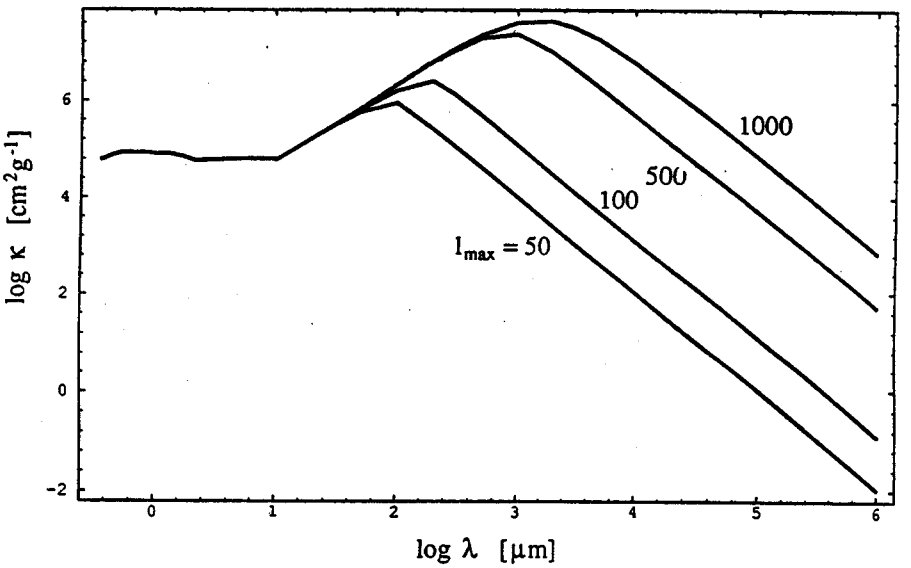

Fig. 1. The mean mass extinction curves for different values of $l_{\max}$, for a wide range of wavelengths.

The relatively flat extinction coefficient from the near UV to near IR shown in Fig. 1 follows from the measured optical constants of iron and is in accord with the data for supernova 1987A.

The arguments of Sec. 2 suggest that $l_{\max} = 1$ mm could arise naturally from the formation process itself. A distribution function defined by (6) with $l_{\max} = 1$ mm may therefore be regarded as a plausible universal distribution of iron whiskers. However, the longest grains are subject to the strongest radiation pressure effects and will tend to be expelled fastest from the vicinity of powerful sources of radiation and indeed from entire galaxies. Whiskers associated with such local sources may therefore have $l_{\max}$ values that are considerably less than 1 mm.

This selective mechanism operates because the main driving mechanism is in the far infrared region with wavelengths of radiation in the range 50–100μm and at these wavelengths the κ-values are higher for longer whiskers. The spectra of most IR-galaxies seem to peak around 100μm and so also does the spectrum of galactic centre region.

4. Galactic Astronomy

4.1. *Supernovae*

(a) *SN1987A*

From day 400 onwards the extinction of the central object of SN1987A over the optical waveband has been found to be insensitive to wavelength, which is in sharp contrast with the strong reddening expected for spherical submicron sized grains

of any composition.[9,10] From Fig. 1 we note that this behaviour is consistent with iron whiskers independent of their lengths. The flat spectrum in the near infrared is also in accord with the thermal re-emission spectrum at around day 800 which is very close to that of a black body.[11] Because it is not expected that the dust shell is optically thick in the waveband 2–15 microns, the whisker model is again to be preferred. Iron whiskers with $l_{\max}$ in the range 50μm to 1 mm could also explain the lack of observed flux in far infrared to microwave wavelength range from (3μm−30cm) in the day 1300 spectrum[12] and also the emission at 1.3 mm observed on day 2172.[13]

(b) *Crab pulsar*

The observations of the Crab Pulsar over a wide range of wavelengths is shown in Fig. 2. We note that a sharp drop in flux occurs both at infrared wavelengths and at millimetre wavelengths. The lack of flux at submillimetre and far infrared wavelengths is fully consistent with a model involving a shell of iron whiskers that surrounds the pulsar. This feature had been highlighted by Arp *et al.*[14]

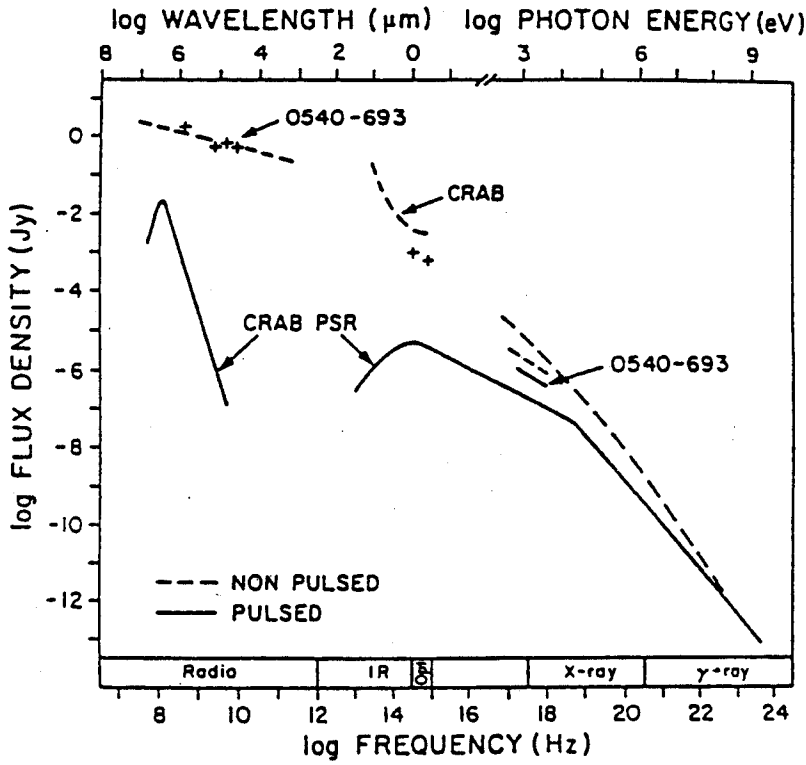

Fig. 2. The spectrum of Crab pulsar shows a significant dip in the wavelength range 30μm to 10 cm. [Source: F. D. Seward *et al.*, in *The Crab Nebula and Related Supernova Remnants*, eds. M. C. Kafatos and R. C. B. Henry (Cambridge, 1985)].

4.2. *Galactic centre*

Recent Gamma-ray observations of the inner galactic centre region appear to indicate that a large number of supernovae ($\sim 10^5$) or a single supermassive object must have exploded there within the last few tens of millions of years.[15,16] Furthermore, intense Fe line emission at 6.7 keV that has been observed within a region $R < 150$ pc shows a clear enhancement of the iron abundance by a factor of up to 2 above solar values.[15] Dame *et al.*[17] show also that the galactic centre Fe line emission is considerably more prominent than the CO line. If the iron is expelled from supernovae in the form of whiskers, the population of such whiskers persisting within the inner galactic centre region for 10^7 yr would be expected to have length distributions truncated to $l_{\max}$ below 100μm.

In this connection we note that Okuda *et al.*[18] have carried out an extensive survey of the CII line emission at 157.7μm of the Galaxy using a balloon borne telescope with a beam resolution of 12′. In the vicinity of the galactic centre, high intensity peaks of this line correspond well with projections of the star-forming annulus at $R = 4$ kpc ($l = 335°$, $l = 25°$) as well as with a much smaller galactocentric region centred on $l = 0$. The overall behaviour across the galaxy of the CII emission is similar to that of the infrared continuum at 12μm, 25μm, 60μm and 157.7μm. A general correspondence of intensity contours at all infrared wavelengths is to be expected on theoretical grounds because the primary energy input for both dust emission and molecular excitation is derived from stellar ultraviolet photons.

A remarkable feature of the CII observations is that the inner core of the galactic centre region, $R < 300$ pc, does not show up as the highest point in contour maps of the $\lambda = 157.7\mu$m line. A similar result was obtained in observations made using the COBE satellite at a coarser beam resolution for both the CII and the NII line at 205.3μm.[19] Both infrared lines showed a clear dip in intensity near $l = 0$. This behaviour for CII contrasts sharply with plots of the far infrared and CO (2.6 mm) emissions. Indeed Okuda *et al.*[18] have found that the deficit in the ratio of CII/FIR emission in the inner core region of the galactic centre may be as large as a factor 3 or 4. A requirement for the iron whisker distribution, if it is to explain the galactic centre data, is that the whiskers retained within $R < 150$ pc can have a high optical depth at 157.7 and 205.3μm, whilst remaining optically thin at 2.6 mm. These conditions are met for $l_{\max} = 100\mu$m, but not for $l_{\max} = 1$ mm.

An alternative explanation of the CII observations has been offered by Nakagawa *et al.*[20] These authors argue that the lower CII line intensities near the galactic centre could be due to an actual reduction of ionizing photons in this region. While this may be a possibility, there is however no compelling reason to support such an hypothesis, and we therefore consider the iron whisker explanation to be far more plausible. Iron whiskers with longer maximal lengths (up to 1 mm) distributed over a more extended region around the galactic inner core could explain the continuum far infrared emission observed by Reach *et al.*[21] and attributed to grains at temperatures in the range 4–7K. Such an extended shell of long whiskers would be required to be optically thin at all far infrared wavelengths.

5. Extragalactic Objects

5.1. *Dust mass requirement in-situ*

Recent observations of millimetre wave radiation from several high redshift sources can also be modelled in terms of a population of iron whiskers retained near these sources. In such instances the average lengths involved may even be less than 100 micrometres.

The models of these sources involve the absorption of high-frequency radiation by a shell of dust which degrades the primary radiation into the far infrared. The emergent radiation is then redshifted into the millimetre waveband due to Hubble expansion. A measured millimetre wave flux S_ν at frequency ν for an object of redshift z corresponds to an intrinsic emission at wavelength $(c/\nu)/(1+z)$. For redshifts in the range $z = 3-5$,[22–24] an observed flux at 1200μm would correspond to a source flux at wavelengths of a few hundred micrometres. Wickramasinghe and Ramadurai[13] have modelled two luminous high redshift objects — BR1202-0725 ($z = 4.69$) and 4C41.17 ($z = 3.8$) — for which good quality data is available, both on the basis of standard grains as well as iron whiskers. For the quasar BR1202-0725 ($z = 4.69$) the flux at wavelength 1100μm is 21mJy, and for the radiogalaxy 4C41.17 ($z = 3.8$) it is 2.5mJy at wavelength 1300μm. In each case the mass of dust required to produce the observed flux values depends on H_0, q_0, the optical properties of dust and the temperature T. Assuming $T = 70$K, $H_0 = 85$ km/s $(\text{Mpc})^{-1}$, $q_0 = 0.5$ the masses required for standard grains and a whisker model are set out in Table 2.

Table 2. Masses of grains in solar masses.

	Iron whiskers	Standard grains
4C41.17	6.65×10^4	7.19×10^7
BR1202-0725	2.31×10^5	2.45×10^8

For standard grains the total mass requirement is seen to be in excess of a few percent of a typical galactic mass. For iron whiskers the masses are nearly 3 orders of magnitude lower, so that the total mass requirement can be seen to be highly conservative and well within plausible limits. For such a model the required dust mass corresponds to the iron yield of some 10^6 type II supernovae.

5.2. *Optical depth of the cosmological medium*

We have already stated that iron whiskers with maximum length of $l_{\max} = 1000\mu$m are very likely to be expelled into extragalactic space. For the consequences of iron whiskers on a cosmological scale we assume therefore the distribution of $n \sim 1/l$ with $10\mu\text{m} \leq l \leq 1000\mu\text{m}$. We now estimate the optical depth produced by the inter-galactic medium out to large redshifts since this will have implications for the observed emission from high redshift objects, especially in the infrared range.

Table 3. Optical depth τ as a function of redshift z and observed wavelength λ for a mixture of iron whiskers $n \sim 1/l$ with $10\mu m \leq l \leq 1000\mu m$.

z	Optical depth τ																		
	λ [μm]																		
	10	20	30	50	100	200	300	500	1000	2000	3000	5000	10000	20000	30000	50000	100000	300000	1000000
.2	.00033	.000948	.00176	.00388	.0118	.0358	.0661	.13	.246	.286	.228	.132	.0461	.013	.00592	.00215	.000542	.0000603	5.43×10^{-6}
.4	.000596	.00172	.00318	.00701	.0212	.0647	.12	.241	.475	.592	.498	.302	.11	.0317	.0145	.00531	.00134	.000149	.0000134
.6	.000824	.00238	.00441	.00968	.0292	.0892	.167	.339	.692	.914	.81	.514	.196	.0579	.0266	.00977	.00246	.000274	.0000247
.8	.00102	.00297	.00549	.012	.0362	.111	.208	.427	.899	1.25	1.16	.771	.307	.0931	.0431	.0159	.00401	.000447	.0000402
1.	.0012	.0035	.00647	.0142	.0425	.13	.244	.507	1.1	1.59	1.53	1.07	.446	.139	.065	.024	.00607	.000678	.000061
1.2	.00137	.00398	.00737	.0161	.0482	.147	.278	.581	1.28	1.94	1.93	1.42	.616	.198	.0932	.0346	.00877	.00098	.0000881
1.4	.00152	.00443	.00821	.0179	.0535	.163	.309	.651	1.46	2.29	2.35	1.81	.822	.271	.129	.0481	.0122	.00137	.000123
1.6	.00167	.00486	.009	.0197	.0585	.178	.338	.715	1.64	2.64	2.79	2.25	1.06	.36	.173	.0651	.0166	.00185	.000167
1.8	.0018	.00525	.00975	.0213	.0632	.192	.365	.777	1.81	3.	3.25	2.73	1.35	.468	.227	.086	.022	.00246	.000221
2.	.00193	.00564	.0105	.0228	.0676	.206	.391	.835	1.97	3.35	3.72	3.24	1.67	.598	.293	.112	.0286	.0032	.000288
2.2	.00206	.006	.0111	.0243	.0719	.219	.415	.891	2.13	3.71	4.2	3.79	2.04	.75	.372	.143	.0366	.00411	.00037
2.4	.00218	.00635	.0118	.0258	.0761	.231	.439	.946	2.28	4.07	4.7	4.39	2.47	.929	.465	.18	.0464	.0052	.000469
2.6	.00229	.0067	.0125	.0272	.0802	.243	.462	.998	2.43	4.43	5.21	5.01	2.94	1.14	.575	.224	.058	.00652	.000587
2.8	.00241	.00704	.0131	.0286	.0841	.255	.485	1.05	2.58	4.79	5.73	5.68	3.47	1.38	.704	.277	.0719	.00809	.000729
3.	.00252	.00737	.0137	.03	.0881	.266	.507	1.1	2.73	5.16	6.28	6.39	4.07	1.66	.855	.339	.0884	.00996	.000898
3.2	.00264	.0077	.0144	.0313	.092	.278	.529	1.15	2.88	5.54	6.84	7.14	4.73	1.98	1.03	.412	.108	.0122	.0011
3.4	.00275	.00804	.015	.0327	.096	.289	.551	1.2	3.03	5.92	7.42	7.94	5.47	2.35	1.24	.498	.131	.0148	.00134
3.6	.00287	.00837	.0156	.0341	.1	.301	.574	1.25	3.19	6.32	8.03	8.79	6.3	2.77	1.48	.6	.159	.018	.00162
3.8	.00299	.00872	.0163	.0356	.104	.313	.596	1.3	3.34	6.73	8.66	9.71	7.22	3.26	1.76	.72	.192	.0217	.00196
4.	.00311	.00908	.0169	.037	.108	.325	.62	1.36	3.5	7.16	9.34	10.7	8.27	3.84	2.09	.863	.231	.0262	.00237
4.2	.00324	.00945	.0176	.0386	.113	.338	.645	1.41	3.67	7.62	10.1	11.8	9.46	4.51	2.48	1.04	.279	.0317	.00286
4.4	.00338	.00986	.0184	.0403	.118	.353	.671	1.48	3.86	8.12	10.9	13.	10.8	5.32	2.96	1.25	.338	.0385	.00348
4.6	.00354	.0103	.0193	.0422	.123	.368	.701	1.54	4.06	8.69	11.8	14.4	12.5	6.32	3.55	1.51	.413	.0471	.00426
4.8	.00373	.0109	.0203	.0445	.13	.387	.737	1.62	4.31	9.37	12.9	16.2	14.6	7.63	4.34	1.87	.514	.0589	.00532
5.	.004	.0116	.0217	.0476	.139	.413	.786	1.74	4.65	10.3	14.5	18.7	17.7	9.64	5.57	2.43	.675	.0774	.00701

We take the quasi-steady state cosmology (QSSC in brief) proposed by Hoyle, Burbidge and Narlikar[25–28] as the relevant cosmological model. The reason for this choice will be made clear in the next section although the results for standard big bang models will not be greatly different. We use the exact solution of the oscillating scale factor obtained by Sachs *et al.*[29] to calculate the optical depth

$$\tau(\lambda, z) = \int_0^z c\rho_0(1+z')^3\kappa\left(\frac{\lambda}{1+z'}\right)\left|\frac{dt}{dz'}\right| dz' . \tag{8}$$

Here λ is the observed wavelength, and ρ_0 is the present density of absorbing matter, which is assumed to be $\rho_0 = 2.5\times10^{-36}$g cm^{-3}. The result for different wavelengths and redshifts is shown in Table 3.

With increasing redshift the maximal τ changes from about $\lambda = 2000\mu$m to $\lambda = 5000\mu$m. For high redshifts, i.e., close to the minimum phase of the oscillation, we have a very large optical depth in the mm-range, whereas the radio and optical ranges, at the right and left end of the table, are only weakly affected.

We will now discuss the implications of Table 3 for two specific cases.

5.3. *The QSO BR 1202–0725*

Wright[30] has raised the issue of optical depth produced by iron whiskers as being excessive. In his paper a mixture of whiskers with length 100μm and 1000μm in a ratio by mass of 50:1 has been used and the present whisker mass density is taken to be 10^{-35} g cm^{-3}.

Wright was concerned in particular with McMahon *et al.*'s[31] observation of the high redshift QSO BR 1202–0725. They detected this QSO with redshift $z = 4.69$ at $\lambda = 1.25$ mm. At such a high redshift, and at this wavelength of observation absorption by iron whiskers is expected to be strong.

Using data given by McMahon *et al.*[31] and Andreani *et al.*[32] we calculated luminosities, optical depth and the necessary increase in luminosities for several QSO's. We have given the big bang (column 4) and the QSSC (column 7) values for comparison. We show the result in Table 4. For redshifts between 3 and 4 the effect is not extremely large. But when we look at $z = 4.69$ there is already a difference of a factor ≈ 240. It is interesting to note that for the two-whisker mixture this factor is about 2500.

The decrease of τ arises due to the following reasons. First, we used the exact solution for the scale factor in QSSC. Previous calculations, especially those criticized by Wright, have been carried out with the approximate solution. Now we could reduce the optical depth for $z = 4.69$ and $\lambda = 1.25$ mm by a factor of 3. Second, we used the more physical distribution of $n \sim 1/l$ instead of the two-whisker model. In the first place this leads to a general increase of τ and a shift of the maximum at a certain redshift towards longer wavelengths. In Sec. 6 we will address the CMB in the context of QSSC. There we will require sufficient optical depth in the wavelength range from a few millimeters to a few centimeters back to $z \approx 5$. This can still be achieved by reducing the present day whisker density to $\rho_0 = 2.5 \times 10^{-36}$g cm^{-3}.

Table 4. Luminosities in BB and QSSC for quasars at $\lambda = 1.25$ mm from (1) Andreani *et al.*[32] and (2) McMahon *et al.*[31]

Quasar	z	F [mJy]	$(\nu L_\nu)_{\rm bb}$ $[h^{-2}L_\odot]$	τ	e^τ	$(\nu L_\nu)_{\rm qssc}$ $[L_\odot]$	Ref.
$2132+0126$	3.19	11.5	1.44×10^{11}	3.67	39.3	1.06×10^{13}	1
$0344+0222$	3.38	5.7	8.11×10^{10}	3.87	47.9	7.44×10^{12}	1
$0345+0130$	3.64	6.1	1.03×10^{11}	4.15	63.2	1.27×10^{13}	1
$0307+0222$	4.38	6.6	1.68×10^{11}	5.02	151	5.45×10^{13}	1
$1202-0725$	4.69	10.5	3.12×10^{11}	5.48	241	1.70×10^{14}	2

Thus, the main point of Wright's criticism that the QSO has to be excessively bright is clearly void in the light of the present work.

5.4. *The ultraluminous infrared galaxy IRAS F10214+4724*

In one of their papers Hoyle *et al.*[26] had considered the ultraluminous IRAS galaxy F10214+4724 with $z = 2.286$. Since its detection by Rowan–Robinson *et al.*[33] this galaxy has caused a great deal of discussion because of its very high luminosity in far infrared. In the rest-frame wavelength range from 6–36μm it is $3 \times 10^{14} L_\odot$, assuming $h = 0.5$, $\Omega = 1$, making F10214+4724 the most luminous IRAS galaxy by a factor of 10.

We will look at the influence of iron whiskers on this galaxy, which is expected to be not very strong, as the redshift is comparably low. Table 5 gives luminosities for big bang and QSSC for wavelengths from 10–61700μm. The maximum effect is at wavelengths of around 1400 mm, where the QSSC luminosity is higher than the big bang luminosity value by a factor 20. As in Table 4 the difference in D_L has been taken into account. The luminosities for the big bang model are given with the parameter h. With a Hubble constant of $h = 0.75$, these values are larger by 1.78.

Recent observations seem to reveal the fact that F10214+4724 is actually a gravitationally lensed galaxy.[34,35,39] With a proposed magnification of about 10, the luminosity in the standard case would be reduced to normal. The probability that it is a lensed system with a magnification of 2 to 10 is about 25%, provided the local luminosity function is valid up to this redshift and luminosity. The probability would considerably increase, if the luminosity function would become steeper at high redshifts. Magnifications of 20 or more are essentially ruled out unless the luminosity function is very steep, $\phi(L) \sim L^{-6}$ or so.[40]

Gravitational lensing does not change the spectrum of the lensed object, unless different parts of the spectrum — e.g., emission lines, radio continuum — originate from different regions of the object, as magnification is a function of the position. Features from small-sized subregions might also be distorted by microlensing. F10214+4724 is said to be an ordinary obscured AGN with the infrared luminosity arising from the obscuring dust torus, a fairly extended region, hence we do not expect significant distortions.

Table 5. Luminosities for different wavelength for IRAS F10124+4724 with flux data from (1) Rowan-Robinson *et al.*,[36] (2) Downes *et al.*,[37] (3) Solomon *et al.*[38]

λ [μm]	F [mJy]	$(\nu L_\nu)_{\rm bb}$ [$h^{-2}L_\odot$]	τ	e^τ	$(\nu L_\nu)_{\rm qssc}$ [$L_\odot$]	Ref.
61700.	0.36	4.32×10^7	0.105	1.11	8.46×10^7	1
35500.	0.27	5.64×10^7	0.303	1.35	1.34×10^8	1
1400.	0.03	1.59×10^8	3.03	20.7	5.79×10^9	3
1200.	9.6	5.93×10^{10}	2.64	14.	1.47×10^{12}	2
1100.	24.	1.62×10^{11}	2.43	11.3	3.22×10^{12}	1
800.	50.	4.63×10^{11}	1.7	5.5	4.48×10^{12}	1
450.	273.	4.5×10^{12}	0.787	2.2	1.74×10^{13}	1
100.	$< 510.$	$< 3.78 \times 10^{13}$	0.0738	1.08	$< 7.17 \times 10^{13}$	1
60.	190.	2.35×10^{13}	0.0331	1.03	4.27×10^{13}	1
25.	$< 90.$	$< 2.67 \times 10^{13}$	0.00867	1.01	$< 4.74 \times 10^{13}$	1
20.	$< 45.$	$< 1.67 \times 10^{13}$	0.00616	1.01	$< 2.96 \times 10^{13}$	1
12.	$< 90.$	$< 5.56 \times 10^{13}$	0.0028	1.	$< 9.82 \times 10^{13}$	1
10.	$< 12.$	$< 8.89 \times 10^{12}$	0.00211	1.	$< 1.57 \times 10^{13}$	1

In the QSSC case the absorption by iron whiskers leads to an additionally required luminosity of a factor 20, especially around 1400μm, where absorption has its maximum.

5.5. *Radio quasars and AGN*

If iron whiskers are expelled from entire galaxies as we have argued, one might hope to find localised absorption effects persisting in the vicinity of systems that have undergone violent episodes of star formation followed by supernovae explosions. In this context one could perhaps turn to "starburst" galaxies and nearby quasars as candidate sites of recent star formation. The spectra of the inner cores of IRAS-detected radio quasars of relatively low redshift (mostly $z \leq 0.5$) studied by Gopal–Krishna and Steppe[41] do indeed show conspicuous dips in their continuum flux near the wavelength of 1.3 mm. The spectra of a representative sample of these sources is reproduced in Fig. 3. The spectra are clearly consistent with absorption by extended localised shells of iron whiskers of millimetre lengths, presumably expelled from the quasar cores. The situation is seen to be comparable to the case of the Crab Pulsar (see Fig. 2).

The high luminosity associated with the cores of such sources would lead to expulsion of whiskers at greatly suprathermal speeds through the ambient gas. Collisions of high-speed whiskers with gas atoms would impart angular momentum transverse to the stream velocity, and hence would lead to alignment of the whisker axes along the stream lines due to the Gold mechanism. The alignment of the iron whiskers would thus be mostly in the radial direction, which would also coincide with the directions defined by a radial magnetic field.

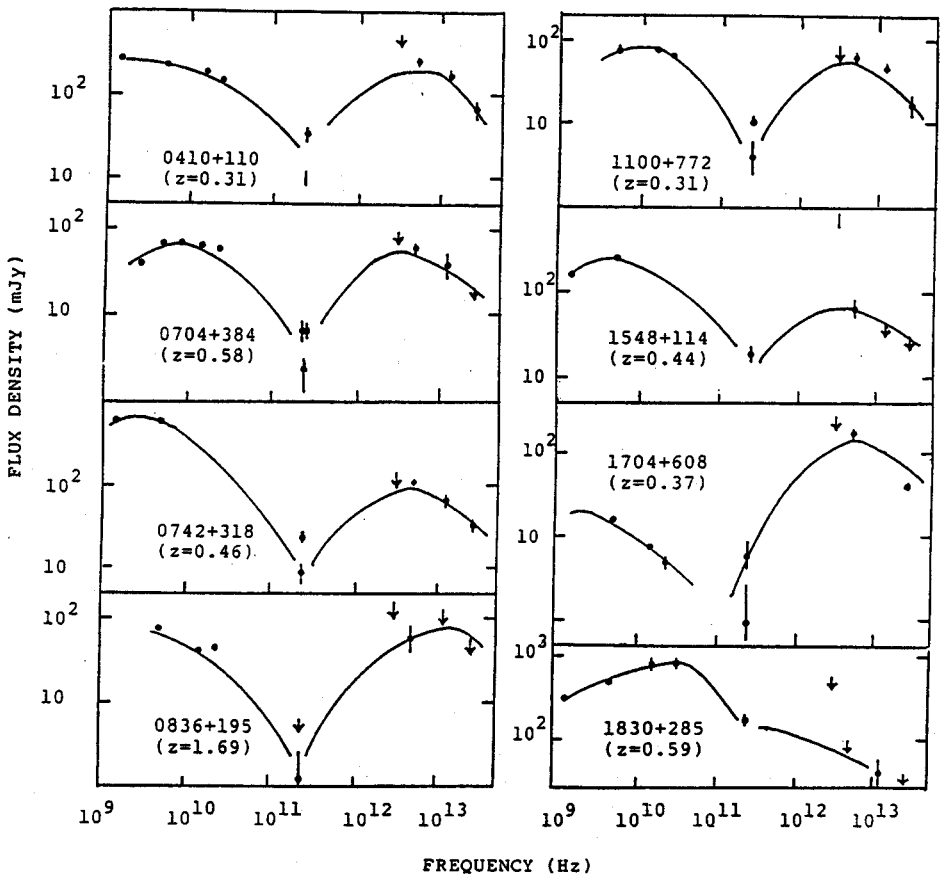

Fig. 3. This figure shows how the flux density of a sample of IRAS-detected radio quasars shows a dip near the wavelength ~ 1.3 mm. Similarity with the Crab quasar curve is significant. Continuous lines have been drawn through the data points of Gopal-Krishna and Steppe (1990).

In a recent review, Miller[42] has drawn attention to the issue of broad line regions (BLR) in Seyfert galaxies like NGC 1068 which still remains unsettled. What causes an opaque region to cover both the BLR and the central source but not the scattering region? This obscuring region is not the accretion disc; indeed there is no evidence to support the existence of an obscuring torus or a disc. Ordinary (spherical) dust grains also do not seem to help. The following scenario may be worth considering in this context.

Imagine a central source with radial magnetic field lines which selectively align the iron whiskers. The radiation from a central region may thus not encounter a wide cross section of whiskers; but that coming out from outer regions would "see" the longer sides of the whiskers. Thus one would not see the scattered BLR which is blacked out by the whiskers. In other words, anisotropy of scatterers may hold the clue to a hitherto unresolved mystery.

6. The Microwave Background

While the applications discussed so far would work in any cosmological model, the whiskers play a crucial role in providing an explanation for the microwave background in the quasi-steady state cosmology (QSSC in brief).

The QSSC was proposed and discussed by Hoyle *et al.* in a series of papers.[25–28] In this cosmology, unlike standard big bang cosmology, there is no unique epoch of "beginning of the universe" with all matter being created at that epoch. Instead the universe is without a beginning and has cycles of expansion and contraction with period Q superposed on a long term exponential trend of expansion with time constant P, with $P/Q \gg 1$. Matter creation is also continuous and periodic; being confined to pockets of strong gravitational fields around compact massive objects. Hoyle *et al.* took the expansion factor of the spacetime as

$$S(t) = \exp(t/P) \cdot \{1 + \eta \cos(2\pi t/Q)\}\,. \tag{9}$$

Here η is a constant in the range $0 < \eta < 1$. This is actually an approximate solution of the field equations derived from a Machian theory of gravity[28] that is a generalized version of the classical general relativity.

This cosmology (QSSC) appears to meet all the available observational constraints at the present time. However, so far as the production of light nuclei and the microwave background is concerned, the QSSC must look for solutions that are radically different from those offered in big bang cosmology. The synthesis of light elements is discussed in the first of the QSSC papers[25] and does not concern us here. An explanation of the microwave background invokes iron whiskers as thermalizing agents of starlight produced by previous generations of stars from earlier cycles. Hoyle *et al.*[26] showed that the energy available from this process is just right to give a radiation background of 2.7K at the present epoch.

The thermalizing mechanism has to satisfy certain constraints, however. It must be efficient enough, i.e., it should have sufficient optical depth to produce a Planckian spectrum for wavelengths shorter than 20 cm. Further, it should be transparent enough to permit optical and radio sources of high redshifts ($z < 5$) to be seen. Recent observations of high redshift quasars at millimetre wavelengths discussed in Sec. 5 also place constraints on the opacity function of the thermalizing agent.

The exact model of Sachs *et al.*[29] referred to in Sec. 5 has the following quantitative specifications. The expansion factor is given by

$$S(t) = \exp\left(\frac{t}{P}\right)[1 + \eta \cos\theta(t)]\,, \tag{10}$$

where $\theta(t)$ is determined by a relation involving the cosmological constant λ:

$$\dot{\theta}^2 = -\frac{\lambda}{(1 + \eta\cos\theta)^2}\{6 + 4\eta\cos\theta + \eta^2(1 + \cos^2\theta)\}\,. \tag{11}$$

There is considerable similarity in character of the exact solution (10) to the approximate solution (9). The oscillatory period Q is given by

$$Q = \frac{1}{\sqrt{-\lambda}} \int_0^{2\pi} \frac{(1+\eta\cos\theta)d\theta}{\{6+4\eta\cos\theta+\eta^2(1+\cos^2\theta)\}^{\frac{1}{2}}} . \tag{12}$$

Thus there is a relationship between the parameters η and Q, through the cosmological constant λ. Notice that λ is negative, i.e., there is a long range force of cosmic attraction.

The interrelationships between P, Q and the cosmological constant λ follow from the field equations which relate the dynamics of quasi-steady expansion and matter creation to the fundamental constants and the number of particles within the sphere defined by the event horizon.

For the computation of Table 3 through formula (8) we have used the following parametric values of Sachs *et al.*[29]:

$$P = 20Q\,, \qquad Q = 4.38 \times 10^{10} \text{ yrs}\,,$$

$$\eta = 0.8\,, \qquad \lambda = -0.29 \times 10^{-56} \text{ cm}^{-2}\,, \qquad t_0 = 0.7Q \text{ (Present epoch)}\,.$$

From this cosmology the following conclusions can be drawn on the basis of Table 3.

1. First we note that at wavelengths 100 m–20 cm sufficient optical depth exists for the radiation to thermalize in twenty cycles (this being the ratio of P to Q). In reading the table note that the present cycle extends backwards to a maximum redshift of 5 so that the absorption in a typical full cycle preceding the present one would correspond to at least twice the value given in the bottom line of the table. Thus the radiation background would be thermalized perfectly over this wavelength range leading to a Planckian spectrum.
2. The optical depths are not significant to block out either radio-astronomy or optical astronomy over the present cycle right upto the maximum redshift. It is possible to "see" even sources from many previous cycles at longer radio wavelengths (21 cm onwards), as well as optical sources of previous cycles. Thus the prediction of QSSC that a few moderately blueshifted sources should be discovered still stands, although these are going to be faint with magnitudes greater than 26.
3. Hoyle *et al.*[43] and we ourselves in this paper (see Sec. 5) have already discussed the issue of whether the microwave emission from high redshift quasars would be visible without unrealistically high demands on their luminosities.

7. Conclusions

We have thus presented what we believe to be a plausible case for the existence of iron whiskers as an important component of the interstellar and intergalactic dust. We have highlighted the model for their production in supernovae which are the

only known sources of iron. The model also leads to a length distribution of these grains with the longer ones being pushed out more readily into intergalactic space. Next we have discussed the possible applications of the whisker model in various settings within the Galaxy and outside it. We have pointed out several observable consequences that can be used to verify the existence of iron whiskers.

We are aware of the credibility gap that might prevent a ready acceptance of whiskers but hope that an objective assessment of evidence will eventually lead to a change of view. We cannot resist, however, a comparison of this idea with another that seems to have encountered very little resistance towards acceptability. Table 6 below gives this comparison.

The reason for the tilt in the opinion towards the right hand column is probably due to the last entry in Table 6.

Table 6. Iron whiskers vs non-baryonic dark matter.

Iron whiskers	Non-baryonic dark matter
Origin is understood in known supernova settings	Origin shrouded in as yet vague theories of particle physics
Condensation of metallic vapours in laboratory shows how whiskers form	No high energy accelerator is able so far to produce evidence for existence of any cold dark matter candidate while the mass of the neutrino, a hot dark matter candidate is still not confirmed by experiments
Iron whiskers have applications in many astrophysical settings involving standard and tested physics	Physical behaviour conjectured and a number of parameters are used to fit structure formation models to make them consistent with the observations of micro-wave background and large scale features of matter distribution so far with no definitive success
Can provide a non-big bang explanation of the microwave background	Badly needed to prop up the big bang theory in the light of data on primordial deuterium, the microwave background and the large scale structure and motion

Acknowledgments

We are grateful to Gopal-Krishna for discussions concerning aspects of AGN and quasars. Rainer Sachs thanks IUCAA for a fellowship that made this work possible. N. C. Wickramasinghe thanks the Exchange Programme between the Indian National Science Academy and the Royal Society for support of his visit to IUCAA.

References

1. F. Hoyle and N. C. Wickramasinghe, *Astrophys. Space Sc.* **147**, 245 (1988).
2. T. Kozasa, H. Hasegawa and K. Nomoto, *Astron. Astrophys.* **249**, 474 (1991).
3. B. Donn and G. W. Sears, *Science* **140**, 1208 (1963).
4. F. R. N. Nabarro and P. J. Jackson, in *Growth and Perfection in Crystals*, eds. R. H. Duramus *et al.* (J. Wiley, New York).
5. G. W. Sears, *Ann. New York Acad. Sci.* **65**, 388 (1957).
6. F. Hoyle and N. C. Wickramasinghe, *The Theory of Cosmic Grains* (Kluwer Academic Press, 1991).
7. N. C. Wickramasinghe, *Light Scattering Functions for Small Particles* (J. Wiley, New York, 1973).
8. N. C. Wickramasinghe, A. N. Wickramasinghe and F. Hoyle, *Astrophys. Space Sc.* **193**, 141 (1992).
9. L. B. Lucy, I. J. Danziger, C. Gouiffes and P. Bouchet, in *Supernovae*, ed. S. E. Woolsey (Springer-Verlag, New York, 1991), p. 82.
10. C. S. J. Pun *et al.*, *Astrophys. J. Suppl.* **99**, 223 (1995).
11. D. H. Wooden *et al.*, *Astrophys. J. Suppl.* **88**, 477 (1993).
12. N. C. Wickramasinghe and A. N. Wickramasinghe, *Astrophys. Space Sc.* **200**, 145 (1993).
13. N. C. Wickramasinghe and S. Ramadurai, *Astrophys. Space Sc.* (1995).
14. H. C. Arp *et al.*, *Nature* **346**, 807 (1990).
15. K. Koyama, H. Awaki, H. Kunieda, S. Takano, Y. Tawara, S. Yamauchi, I. Hatsukade and F. Nagase, *Nature* **339**, 603 (1989).
16. K. Koyama and S. Yamauchi, *Astrophys. J.* **404**, 620 (1993).
17. Dame *et al.*, *Astrophys. J.* **322**, 706 (1987).
18. H. Okuda, T. Nakagawa, H. Shibai, Y. Doi, Y. Y. Yui, K. Mochizuki, T. Nishimura and F. J. Low, *Astrophys. J.* **455**, L35 (1993).
19. C. L. Bennett and G. Hinshaw, *AIP Conf. Proc.* **278**, 257 (1993).
20. T. Nakagawa, Y. Doi, Y. Y. Yui, H. Okuda, K. Mochizuki and H. Shibai, *Astrophys. J.* **455**, L35–38 (1995).
21. W. T. Reach *et al.*, *Astrophys. J.* **451**, 188 (1995).
22. J. S. Dunlop *et al.*, *Nature* **370**, 347 (1994).
23. K. G. Isaak, R. G. McMahon, R. E. Hills and S. Withington, *Mon. Not. R. Astron. Soc.* **269**, L28 (1994).
24. R. Chini and E. Krugel, *Astron. Astrophys.* **288**, L33 (1994).
25. F. Hoyle, G. Burbidge and J. V. Narlikar, *Astrophys. J.* **410**, 437 (1993).
26. F. Hoyle, G. Burbidge and J. V. Narlikar, *Mon. Not. R. Astron. Soc.* **267**, 1007 (1994).
27. F. Hoyle, G. Burbidge and J. V. Narlikar, *Astron. Astrophys.* **289**, 729 (1994).
28. F. Hoyle, G. Burbidge and J. V. Narlikar, *Proc. Roy. Soc.* **A448**, 191 (1995).
29. R. Sachs, J. V. Narlikar and F. Hoyle, *Astron. Astrophys.* **313**, 703 (1996).
30. E. L. Wright, *Mon. Not. R. Astron. Soc.* **276**, 1421 (1995).
31. R. G. McMahon *et al.*, *Mon. Not. R. Astron. Soc.* **267**, L9 (1994).
32. P. Andreani, F. LaFranca and S. Cristiani, *Mon. Not. R. Astron. Soc.* **261**, L35 (1993).
33. M. Rowan-Robinson *et al.*, *Nature* **351**, 719 (1991).
34. T. Broadhurst and J. Lehár, *Astrophys. J.* **450**, L41 (1995).
35. J. R. Graham and M. C. Liu, *Astrophys. J.* **449**, L29 (1995).
36. M. Rowan-Robinson *et al.*, *Mon. Not. R. Astron. Soc.* **261**, 513 (1993).
37. D. Downes *et al.*, *Astrophys. J.* **398**, L25 (1992).
38. P. M. Solomon, D. Downes and S. J. E. Radford, *Astrophys. J.* **398**, L29 (1992).
39. S. Serjeant *et al.*, *Mon. Not. R. Astron. Soc.* **276**, L31 (1995).

40. N. Trentham, *Mon. Not. R. Astron. Soc.* **277**, 616 (1995).
41. Gopal-Krishna and H. Steppe, in *Variability of Active Galactic Nuclei*, eds. J. S. Miller and Witta, GSU Conference (1990).
42. J. S. Miller, in *The Physics of Active Galaxies*, eds. G. V. Bicknell *et al.*, *APS Conference Series* **54**, 149 (1994).
43. F. Hoyle, G. Burbidge and J. V. Narlikar, *Mon. Not. R. Astron. Soc.* **277**, L1 (1995).